Title

Electron density enhancement over a wide altitude range during ionosphere heating experiments at EISCAT

Authors and affiliations

(1) Jun Wu[1], (email: wujun1969@163.com)

(2) Jian Wu[1],

(3) Jie Feng[1,2],

(4) Qingliang Li[1],

(5) Shuji Hao[1],

(6) Zhengwen Xu[1],

(7) Haisheng, Zhao[1].

[1]National Key Laboratory of Electromagnetic Environment, China Research Institute of Radio Wave Propagation, Beijing 102206, China

[2]School of Physics, Xidian University, Xi'an, 710071, China

Key Points

(1) Whether the apparent enhancement corresponds to a true enhancement in electron density.

(2) Following the dispersion relation of ion acoustic waves, two observations are analyzed.

(3) The apparent enhancement was falsified.

Plain Description

Above the reflection altitude of the high-frequency pump wave, an apparent electron density enhancement was observed during two ionospheric heating experiments conducted on 18 Oct. 2012 and 11 Mar. 2014 respectively. Those observations seem to be in conflict with the understanding that the high-frequency pump wave should be reflected at the reflection altitude, so that the ionosphere plasma should not be modificated above the reflection altitude of the high-frequency pump wave. One needs to verify the validity of this enhancement. No significant modifications were found in the electron temperature and ion line frequency, post the comparison of the enhanced ion line and the background ion line. According to the dispersion of ion acoustic waves, this implies that no change occurred in the effective ion mass. Furthermore, the incident radiation and the drift velocity did not indicate a significant change in the ion species and their densities. Thus, the electron density did not truly change over the wide altitude range.

Abstract

During the course of ionospheric heating experiments, an apparent electron density enhancement was observed at the European Incoherent Scatter Scientific Association (EISCAT). The enhancement extended over a wide range of altitudes, above the reflection altitude of the high-frequency pump wave. However, it remains open whether this enhancement actually corresponds to a true enhancement in electron density. Following the dispersion relation of ion acoustic waves, the frequency ratio of the enhanced ion line to the background ion line suggests that the profile of the effective ion mass might remain unchanged. Furthermore, the solar radio flux and ion drift velocity indicated no significant changes in the ion species and their densities. In conclusion, the electron density enhancement observed at EISCAT, might not in fact be a true enhancement.

1. Introduction

In the F region of the ionosphere (altitudes >160 km), powerful high-frequency (HF) pump waves can regularly induce an appreciable change in electron density in the vicinity of the HF pump wave reflection altitude. Some typical studies in the past have observed/theorised such electron density modifications. *Utlaut* and *Violette* [1972] inferred a ~7% decrease in the electron density from ionograms recorded at the Platteville Atmospheric Observatory, Colorado, USA (henceforth referred to as Platteville). Later, using the typical parameters at the Arecibo Observatory, Puerto Rico (henceforth referred to as Arecibo) and Platteville, *Meltz et al*. [1974] suggested a theoretical decrease of ~3% in electron density, two minutes post the onset of HF pumping. Experiments by *Djuth et al.* [1987] at Arecibo demonstrated that a decrease of ~10–15% in the electron density was accompanied by a 1000–2000 K increase in the electron temperature. *Duncan et al*. [1988] reported the first thermally driven decrease of ~50% in electron density. However, the observations at the European Incoherent Scatter Scientific Association (EISCAT) showed both an increase and decrease in the electron density in the vicinity of the reflection altitude of the HF

pump wave, demonstrating disagreements with a time-dependent numerical model [*Stocker et al*., 1992]. At the High Frequency Active Auroral Research Program (HAARP), *Pedersen et al.* [2010, 2011] observed a large enhancement in electron density at the altitude of ~220 km induced by the HF pump wave near the 2nd electron gyroharmonic.

In recent years, an apparent enhancement in the electron density, induced by HF pump waves in X mode [*Senior et al*., 2013] and O mode [*Wu et al.*, 2016, 2017], was observed over a wide range of altitudes above the pump wave reflection altitude. *Senior et al*. [2013] found that the shape of the enhanced ion line corresponded very closely with that of the ion line taken before the onset of pumping at the altitude of ~300 km, and that the frequency of the plasma line showed no appreciable change at the altitudes of ~321 km and ~339 km. It was concluded that the apparent enhancement did not in fact correspond to a true enhancement in electron density. Instead, it corresponded to the enhanced ion line by some unknown mechanisms, which preferentially scatters the radar wave back along the magnetic field line. *Rietveld et al.* [2020] proposed that medium and large-scale field-aligned irregularities could refract the radar wave along the magnetic field. This may cause a strong radar backscatter, appearing in the observation as an enhanced electron density. However, *Blagoveshchenskaya et al*. [2022] claimed that this apparent enhancement did correspond to a true enhancement in electron density and might be due to an increased ionization resulting from the flux of accelerated electrons. It was expected that the duct of the enhanced electron density may guide the HF pump wave along the magnetic field line. Indeed, the debate continues over the apparent or true nature of this enhancement in the electron density, and the conclusive proofs are still expected.

It is essential to confirm the apparent or true nature of the ionospheric electron density enhancement, on which the research path of physical mechanisms heavily depends. That is, if the apparent enhancement does in fact correspond to a true enhancement in electron density, the research of physical mechanisms will focus on the interaction between the HF pump wave and the ionospheric plasma, otherwise it should focus on the scattering process of radar wave.

In this paper, an alternative method, confirming the apparent or true nature of the ionospheric electron density enhancement, is presented, and two ionospheric heating experiments are examined.

2. Experiment and Data

At EISCAT, near Tromsø, Norway (69.58°N, 19.21°E), the heating facility can radiate an O / X mode HF pump wave in the frequency range of 4.0–8.0 MHz [*Rietveld et al.*, 1993]. It also hosts an ultra-high frequency (UHF) incoherent scatter radar (ISR), operating at 930.0 MHz [*Rishbeth* and *van Eyken*,1993]. In this study, we examined two experiments involving the aforementioned heating facility and UHF ISR:

1) The first experiment (henceforth referred to as Experiment 1) was conducted by *Senior et al.* [2013] on 18 October 2012, between 13:10–14:50 universal time (UT). The heating facility was operated at 7.953 MHz, pointing in the field-aligned direction (12° with the zenith, 186° with the azimuth), and with an effective radiated power (ERP) of ~840.0 MW. The HF pump wave was modulated to stay on for 300 s, followed by a break of 300 s, with the polarization switching between the O and X modes on successive pulses, making an overall cycle of 1200 s. The radar beam began in the field-aligned direction for the first 120 s, followed by an alignment of 11° and 13° with the zenith for 60 s each. Finally, the radar beam was returned to the field-aligned direction for 60 s before turning off the HF pumping. The radar power was measured at ~1.5 MW, with the HF pumping on, and at ~1.6 MW, after turning it off.

2) The second experiment (henceforth referred to as Experiment 2) was conducted by *Wu et al.* [2016, 2017] on 11 March 2014, between 12:30–14:30 UT. The heating facility was operated at frequencies in steps of 2.8 kHz, starting from 6.7 MHz to 7.0 MHz. The ERP had a range of 56.0–78.0 MW. The O mode HF pump wave was modulated to stay on for 18 min, and then, off for 12 min. The radar beam and HF pump beam stayed in the field-aligned direction throughout the experiment. The radar

power was measured at ~1.4 MW, with the pumping on, and at ~1.5 MW after turning it off.

In addition, *Senior et al.* [2013] and *Wu et al.* [2016, 2017] gave a detailed description of the two experiments, in which more experimental information is available. To allow ion line smoothing, the ISR data was analyzed using an integration time of 60 s in this study.

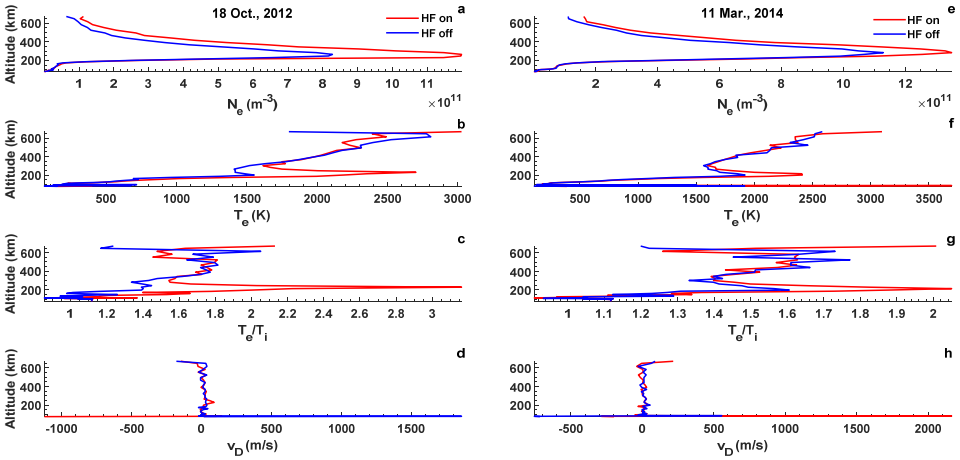

Figure 1. (a) Mean electron density; (b) mean electron temperature; (c) mean ratio of electron temperature to ion temperature; and (d) mean ion drift velocity measured in Experiment 1. Each enhanced (red) / background (blue) value is the mean of the integration of the X-mode pump wave, over the final 60 s of the on/ off period, for five cycles. Subplots (e), (f), (g), and (h) correspond to (a), (b), (c), and (d), respectively, for Experiment 2. The description follows in Experiment 1, but measured only over three on/ off cycles. The values were obtained using Grand Unified Incoherent Scatter Design and Analysis Package (GUISDAP) [*Lehtinen and Huuskonen*, 1996].

Figure 1 displays the mean electron density N_e, mean electron temperature T_e, mean ratio of electron temperature to ion temperature $\frac{T_e}{T_i}$, and mean ion drift velocity v_D. It can be seen that with the HF pumping on, N_e, T_e and $\frac{T_e}{T_i}$ increase significantly in the narrow altitude range of ~200–300 km. This was attributed to (i) the weak leakage of the X mode pump wave into the O mode by *Senior et al.* [2013], and (ii) the HF enhanced ion line and upper hybrid resonance close to the reflection altitude of the HF pump wave by [*Wu et al.*, 2017]. However, there exists no evidence of a significant change in v_D, i.e., the drift of ionosphere plasma was not active in the

geomagnetic field-aligned direction. In both cases, an unexpected enhancement of ~20–50% was observed in N_e above ~300 km, till the altitude limit of the radar measurement. This was consistent with the clear enhancement in the ion lines within the altitude range of ~245–486 km, as illustrated in Figure 2.

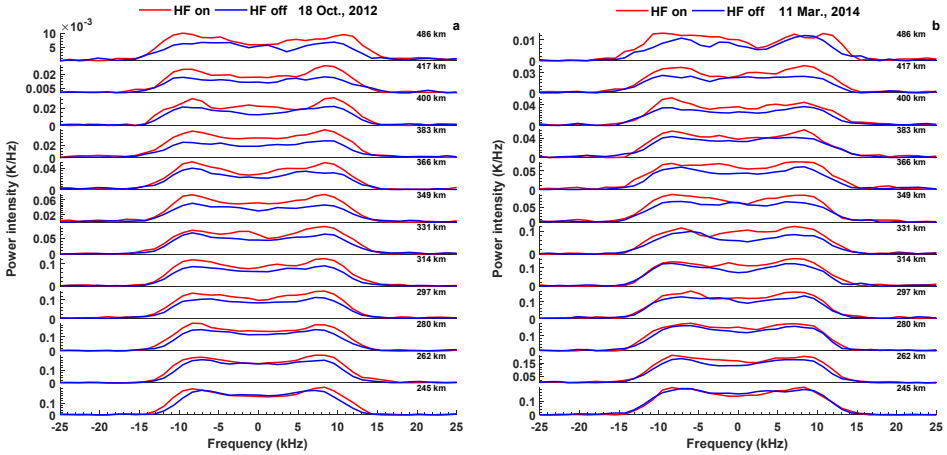

Figure 2. (a) Examples of ion lines measured in Experiment 1; (b) Examples of ion lines measured in Experiment 2. The ion lines were obtained using the EISCAT Real Time Graphic (RTG) package. The ion lines above the altitude of ~500 km were not shown due to the smaller signal to noise ratio (SNR) of the ISR echo. Additionally, the ion line measurement follows the same method as that in Figure 1.

Figure 2 illustrates examples of ion lines in the altitude range of ~245–~500 km for both experiments. It is evident that in both cases, when the pumping is on, the ion lines at ~9.5 kHz are significantly enhanced in intensity. Based on the standard analysis of incoherent scatter, this observation indicates that the profile of electron density N_e should be modified by the HF pumping. Moreover, the intensity of the ion lines, below the altitude of ~314 km, are an order of magnitude more intensive than that above the altitude of ~314 km, i.e., depending on the N_e profile and the radar echo scattered from the scattering volume.

To summarize, as observed in Figures 1 and 2, an interesting enhancement is seen in N_e and the ion lines in the altitude range of ~300–500 km, when the HF pumping is on.

3. Discussion

It is assumed that the ionosphere plasma remains Maxwellian during the ionospheric heating experiments, and the GUISDAP and the RTG are valid for the ionosphere plasma illuminated by the HF pump. The assumption is based on four factors, namely, (i) the HF pump wave should be reflected at its reflection altitude [*Robinson,* 1989], and the ionosphere plasma should not be disturbed by the HF pump and should remain Maxwellian; (ii) only N_e was enhanced, whereas other parameters remained unchanged; (iii) if the apparent enhancement does not in fact correspond to a true enhancement in electron density, the ionosphere plasma should indeed remain Maxwellian; and (iiii) the parameters and ion lines in section (2) were obtained using the GUISDAP and the RTG, which are based on the standard incoherent scatter analysis.

For $\frac{T_e}{T_i} \le 4$, the incoherent backscattered power P_r can be expressed as [*Evans*, 1969; *Djuth et al.,* 1987; *Duncan et al.*, 1988]

$$P_r \propto N_e \sigma_e \left(1+\frac{T_e}{T_i}\right)^{-1}, \quad (1)$$

where σ_e is the Thomson cross section for electrons. In Figures 1(c) and 1(g), $\frac{T_e}{T_i}$ shows no appreciable change in the altitude range of ~300–500 km in either experiment, implying that the ion lines in Fig. 2 were enhanced only as a result of the enhanced N_e, as indicated by Equation (1). On the other hand, N_e is enhanced solely because of the enhanced ion line, as indicated by the standard analysis of incoherent scatter. Thus, the enhanced N_e is equivalent to the enhanced ion line, that is, there is a closed relationship between the enhanced N_e and the enhanced ion line, which satisfies the incoherent scatter theory. Obviously, for confirming the apparent or true nature of the enhanced N_e, examining ion line intensity gets invalid. Hence, instead of ion line intensity, we will examin ion line frequency.

For the quasi-neutral F region of the ionosphere, an ion acoustic wave should

satisfy [*Robinson,* 1989; *Kohl et al.,* 1993; *Alcaydé,* 1995]

$$\omega_i^2 = K_B \frac{\gamma T_i + T_e}{M_i} k_i^2, \quad (2)$$

where ω_i, k_i, γ, K_B, and M_i denote the angular frequency, wave number, adiabatic index, Boltzmann constant, and effective ion mass, respectively. In the case of backscatter, the ISR can only observe an ion acoustic wave satisfying the Bragg condition $k_i = 2k_r$, where k_r denotes the wave number of ISR, and has a value of 19.5 m^{-1} for the UHF ISR at EISCAT. This implies that all the ion lines, observed in Experiments 1 and 2 (Figure 2**)**, satisfy the Bragg condition. In other words, $k_i = 39\ m^{-1}$ is a constant for all examined ion lines, although those ion acoustic waves within a small range of $2k_r$ may also contribute [*Hagfors*, 2003]. Moreover, in both the experiments, the profiles of T_e and $\frac{T_e}{T_i}$ are independent of the HF pumping in the altitude range of ~300–500 km (Figures 2(b), 2(c), 2(f) and 2(g)), i.e., although there exist some natural variability in T_e and $\frac{T_e}{T_i}$, they can still be considered to have a quasi-constant profile in the altitude range of interest. Thus, the straightforward relation between ω_i and M_i is obtained as

$$\omega_i^2 = \frac{\alpha}{M_i}, \quad (3)$$

where $\alpha = \left(\frac{\gamma}{T_e/T_i} + 1 \right) K_B T_e k_i^2$ is a quasi-constant profile in the altitude range of interest.

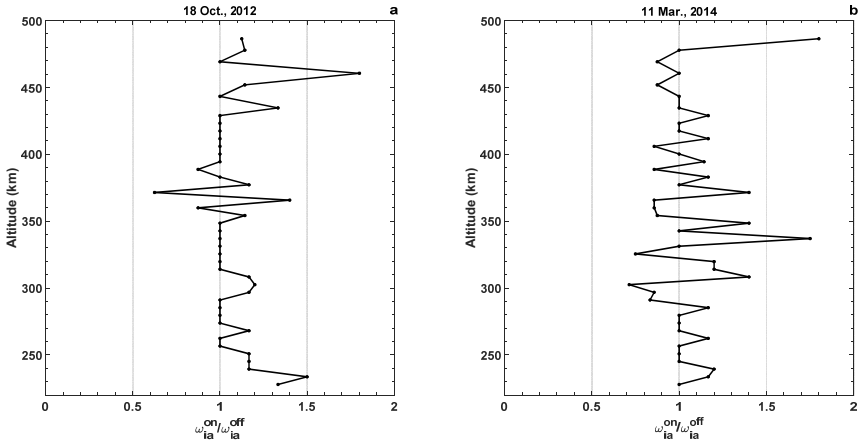

Figure 3. (a) Ratio of the enhanced ion line frequency to the background ion line frequency, measured in Experiment 1; (b) Same ratio as in (a) for Experiment 2, where the frequency is the value corresponding to the maximum intensity of the right shoulder of the ion line.

Equation (3) indicates that, throughout the experiments, the profile of ω_i is dependent on that of M_i, namely, the change in ω_i should be dependent on the change in M_i. Figure 3 demonstrates the ratio of the enhanced ion line angular frequency ω_i^{on} to the background ion line angular frequency ω_i^{off} as a function of the altitude. Note that the SNR of this ratio in Experiment 1 is obviously larger than that in Experiment 2 (Figure 3). This may be the result of (i) the higher number of observation cycles in Experiment 1 (five cycles) over Experiment 2 (three cycles); and the higher radar power, with pumping on, in Experiment 1 than Experiment 2, i.e., the radar echo may have been more intense during Experiment 1.

From Figure 3(a), we can observe that $\frac{\omega_i^{on}}{\omega_i^{off}}$ has a mean of ~1.03 in the altitude range of ~270–450 km, implying that the ion line frequency was not significantly changed by the HF pumping in Experiment 1. Thus, following Equation (3), $\frac{M_i^{off}}{M_i^{on}}$ has a mean of ~1.06 in the altitude range of ~270–450 km, where M_i^{on} denote the effective ion mass with the pumping on, and M_i^{off} denote the effective ion mass with the pumping off. This implys that M_i was not significantly changed by the HF

pumping in the altitude range of ~270–450 km. However, below the altitude of ~270 km, $\frac{\omega_i^{on}}{\omega_i^{off}}$ has a mean of ~1.2. This change could be attributed to the natural ion acoustic waves close to ω_i^{on}. Here, for distinguishing from the high-frequency enhanced ion acoustic waves by the parametric decay instability, the natural ion acoustic waves denote the waves unaffected by the HF pump wave. The natural ion acoustic wave covers a wide frequency spectrum due to the highly varied ion mass distribution in the ionosphere, with some of the higher frequencies satisfying the Bragg condition, as T_e enhances in the scattering volume below the altitude of ~270 km. In other words, following Equation (2) and considering a constant M_i, when T_e becomes higher in the scattering volume, the ion acoustic waves at the higher frequencies will be observed, so that $\frac{\omega_i^{on}}{\omega_i^{off}} > 1$ below the altitude of ~270 km; for instance, at the altitude of ~230 km, $\frac{T_e^{on}}{T_e^{off}} \approx 2.27$ in Figures 1(b) and $\frac{\omega_i^{on}}{\omega_i^{off}} \approx 1.50$ in Figures 3(a), where T_e^{on} denotes the electron temperature with the pumping on and T_e^{off} denotes the electron temperature with the pumping off. The measurement error, resulting from the small SNR, may lead to the increased frequency ratio mean value of ~1.24 above the altitude of ~450 km. Indeed, Equation (1) indicates that P_r must reduce above the altitude of ~450 km due to the decreasing N_e and increasing $\frac{T_e}{T_i}$, as shown in Figure 1. Similarly, the above behavior holds true for Experiment 2, namely, $\frac{\omega_i^{on}}{\omega_i^{off}}$ has a mean of ~1.04 in the altitude range of ~270–450 km, ~1.05 below the altitude of ~270 km and ~1.4 above the altitude of ~450 km, as shown in Figure 3(b). It is important to note that in the altitude range of ~270–450 km, although the intensity of the ion lines is enhanced when the HF pumping is on, their frequency

258 remains unchanged. This implies that the M_{i} profile may remain unchanged in the
259 altitude range of ~270–450 km.

260 Now, M_{i} can be expressed as

261 $$M_{\mathrm{i}} = \frac{1}{N_{\mathrm{e}}} \sum_{\mathrm{i}} N_{\mathrm{i}} m_{\mathrm{i}} , \tag{4}$$

262 where N_{i} and m_{i} denote the density and mass of ion species, respectively. The
263 quantity $N_{\mathrm{i}} m_{\mathrm{i}}$ is dependent on the incident radiation and the atmospheric
264 composition, regardless of the corpuscular ionization which may be significant in the
265 nighttime ionosphere [*Rishbeth* and *Owen*, 1969]. With a constant profile of
266 atmospheric composition, a strong incident radiation could lead to an increase in N_{i}.
267 As the indices of solar activity [*Nicolet* and *Bossy*, 1985], solar radio fluxes (SRFs)
268 were measured at 245.0, 410.0, 610.0, 1415.0, 2695.0, 4995.0, 8800.0, and 15400.0
269 MHz, as shown in Figure 4. With the exception at 610.0 MHz, the SRFs do not
270 demonstrate a significant and systematic variation in intensity during either
271 experiment. At 610.0 MHz, the intensity of the SRF varied between ~10000–140000
272 solar flux units (SFU) in Experiment 1 and Experiment 2. Obviously, the SRFs do not
273 temporally synchronize with the enhanced N_{e}. Also, the HF pump wave was
274 reflected at the altitude of ~240 km and ~230 km for Experiments 1 and 2,
275 respectively. Thus, in both experiments, it is reasonable to assume that the incident
276 radiation does not have a significant impact on N_{i}.

277 Moreover, an analysis of the vertical drift of plasma, in both experiments shows
278 that $v_{\mathrm{D}} \approx 0$, indicating no active drift of plasma along the magnetic field lines,
279 suggesting no induced change in the ion species. Nevertheless, a further examination
280 of the change in ion species should be necessary. The ionosphere is mainly composed
281 of hydrogen ion H^+, helium ion H_e^+, nitrogen ion N^+, atomic oxygen ion O^+,
282 molecular oxygen ion O_2^+ and nitric oxide ion NO^+ in the altitude range of interest

[*Robinson,* 1989]. The frequency of the ion acoustic wave corresponding to H^+ is $\frac{k_r}{2\pi}\sqrt{\gamma\frac{K_B T_e}{m_{iH^+}}} \approx 43.7$ kHz, where k_r=39 m^{-1} for the UHF radar, γ denotes adiabatic index, K_B denotes Boltzmann constant, m_{iH^+} denotes mass of H^+, T_e is ~2000 K as given in **Figure (1)**. This indicates that the frequency of the ion acoustic wave corresponding to H^+ does not lie in the ion line channel of [-40kHz, 40kHz] of UHF ISR at EISCAT, implying that the ion acoustic wave corresponding to H^+ cannot be collected by the UHF ISR. Similarly, the frequency of the ion acoustic wave corresponding to H_e^+ is ~ 22 kHz, which significantly deviate from ~ 9.5 kHz shown in **Figure 2**. The frequencies of the ion acoustic waves corresponding to N^+, O^+, O_2^+ and NO^+, respectively, are ~ 11.5 kHz, ~10.5 kHz, ~7.8 kHz and ~8 kHz, all of which may contribute to the ion lines at ~9.5 kHz shown in **Figure 2**. Considering that the frequencies of ion lines have no significant change in **Figure 2**，the ion species of N^+, O^+, O_2^+ and NO^+ may not have been modified in the altitude range of interest. Both these analyses strongly imply no modification has occurred in the ion species.

As a result, a straightforward relation between M_i and N_e can be obtained as,

$$M_i = \frac{\beta}{N_e}, \tag{5}$$

where $\beta=\sum_i N_i m_i$ is a quasi-constant profile. Equation (5) indicates that, during the course of both experiments, since no modifications occurred in M_i , N_e must also not have been enhanced by the HF pumping in the altitude range of ~270–450 km.

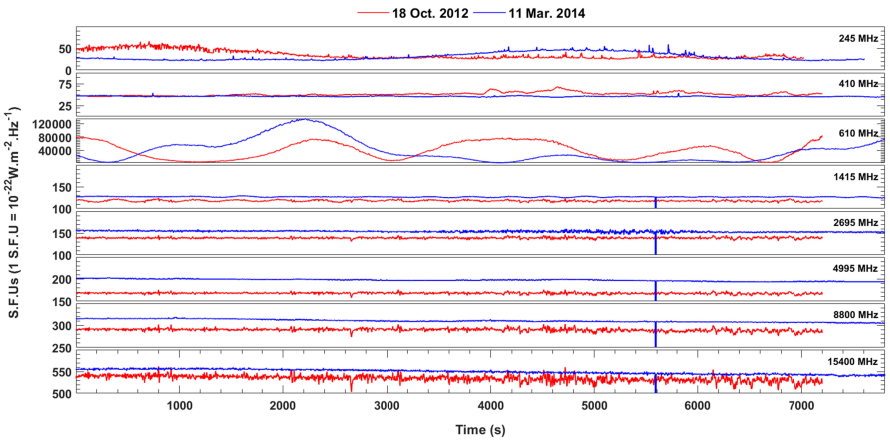

Figure 4. SRF above baseline as recorded at the Radio Solar Telescope Network radio observatory in San Vito, Italy. The abscissa origin denotes 13:00:00 UT on 18 October 2012 (Experiment 1) and 12:20:00 UT on 11 March 2014 (Experiment 2).

4. Summary

With regard to the apparent enhancement in electron density over a wide altitude range during the ionospheric heating experiments, the observations at EISCAT are investigated by following the dispersion relation of ion acoustic waves.

Our investigation showed no significant modifications in the ion line frequency and the electron temperature in the altitude range of interest, strongly implying that the profile of the effective ion mass must remain unchanged. Moreover, the incident radiation and the ion drift velocity indicate that the ion species and their densities must not have been modified. With the assumption of quasi-neutrality, it can be reasonably concluded that the apparent electron density enhancement does not in fact correspond to a true enhancement in electron density.

Acknowledgments

The authors thank the editor and the anonymous reviewers for their constructive and helpful comments, UK colleagues for their significant efforts in the experiment, National Centers for Environmental Information for providing the SRF data, and Dr. Ingemar.Haggstrom for the fruitful discussion about EISCAT data. EISCAT is an international association supported by research organizations in China (CRIRP),

Finland (SA), Japan (NIPR and STEL), Norway (NFR), Sweden (VR), and the United Kingdom (NERC). Dr. Xu is supported by the Taishan Scholars Project of Shandong Province under Grant ts20190968.

Open Research

Data Availability Statement: The ISR and SRF data, respectively, are available for free and public download at https://portal.eiscat.se/schedule/ and https://www.ngdc.noaa.gov/stp/space-weather/solar-data/solar-features/solar-radio/rstn-1-second/.

References

Blagoveshchenskaya N. F., Borisova, T. D., Kalishin, A. S., Egorov, I. M., & Zagorskiy, G. A., (2022). Disturbances of electron density in the high latitude upper (F-region) ionosphere induced by X-mode HF pump waves from EISCAT UHF radar observations. *Arctic and Antarctic Research*, **68**(3), 248-257. http://doi.org/10.30758/0555-2648-2022-68-3-248-257

Denis Alcaydé (1995). Incoherent scatter. *Theory, Practice and Science*. (Technical Report 97/53, pp 33 – 66). Kiruna, Sweden: EISCAT Scientific Association.

Djuth, F. T., Thidé, B., Ierkic, H.M. & Sulzer, M. P. (1987). Large F-region electron temperature enhancements generated by high-power HF radio waves. *Geophys. Res. Lett*., **14**(9), 953-956. http://doi.org/10.1029/GL014i009p00953

Duncan, L. M., Sheerin, J. P. & Behnke, R. A. (1988). Observations of ionospheric cavities generated by high-power radio waves. *Phys. Rev. Lett*., **61**(2), 239-242. http://doi.org/10.1103/PhysRevLett.61.239

Evans, J.V.. (1969). Theory and practice of ionosphere study by Thomson scatter radar. *Proceedings of the IEEE*. **57**(4). 496 - 530. https://doi.org/10.1109/PROC.1969.7005

Hagfors T. (2003). Basic physics of incoherent scatter. *EISCAT summer school* 2003, SRI, Menlo Park CA, Auguest, 2003.

Kohl, H., Kopka, H., Stubbe, P. & Rietveld, M. T. (1993). Introduction to ionospheric heating experiments at Tromso-II. Scientific problems. *J. Atmos. Terr. Phys*., **55** (4/5), 601-613. http://doi.org/10.1016/0021-9169(93)90008-M

Lehtinen, M. & Huuskonen, A. (1996). General incoherent scatter analysis and GUISDAP. *J. Atmos. Terr. Phys*., **58**(1-4), 435-452. http://doi.org/10.1016/0021-9169(95)00047-X

Marcel Nicolet & Lucien Bossy (1985). Solar radio fluxes as indices of solar activity. *Planetary and Space Science*, **33**(5), 507-555. http://doi.org/10.1016/0032-0633(85)90096-0

359 Meltz, G., Holway Jr. L. H. & Tomljanovich, N. M. (1974). Ionospheric heating by
360 powerful radio waves. *Radio Sci.*, **9**(11), 1049-1063.
361 http://doi.org/10.1029/RS009i011p01049
362 Pedersen, T., Gustavsson, B., Mishin, E., Kendall, E., Mills, T., Carlson, H. C. &
363 Snyder, A. L. (2010). Creation of artificial ionospheric layers using high-power HF
364 waves. *Geophys. Res. Lett*., **37**(2), L02,106. http://doi.org/10.1029/2009GL041895
365 Pedersen, T., McCarrick, M., Reinisch, B., Watkins, B., Hamel, R. & Paznukhov, V.
366 (2011). Production of artificial ionospheric layers by frequency sweeping near the
367 2nd gyroharmonic. *Ann. Geophys*., **29**(1), 47-51.
368 http://doi.org/10.5194/angeo-29-47-2011
369 Rietveld, M. T. & Senior, A. (2020). Ducting of incoherent scatter radar waves by
370 field-aligned irregularities. *Ann. Geophys.*, **38**(5), 1101-1113.
371 http://doi.org/10.5194/angeo-38-1101-2020
372 Rietveld, M. T., Kohl, H., Kopka, H. & Stubbe, P. (1993) Introduction to ionospheric
373 heating at Tromsø-I. Experimental overview. *J. Atmos. Terr. Phys*., **55**(4/5),
374 577-599. http://doi.org/10.1016/0021-9169(93)90007-L
375 Rishbeth, H. & Owen, K. (1969). Introduction to Ionospheric Physics. *Academic*
376 *Press*, New York
377 Rishbeth, H. & Van Eyken, A. (1993). EISCAT: early history and the first ten years of
378 operation. *J. Atmos. Terr. Phys.*, **55**(4-5), 525-542.
379 http://doi.org/10.1016/0021-9169(93)90002-G
380 Robinson, T. R. (1989). The heating of the high latitude ionosphere by high power
381 radio waves. *Physics Reports*, **179** (2/3), 79-209.
382 http://doi.org/10.1016/0370-1573(89)90005-7
383 Senior, A., Rietveld, M. T., Häggström, I. & Kosch, M. J. (2013). Radio-induced
384 incoherent scatter ion line enhancements with wide altitude extents in the
385 high-latitude ionosphere. *Geophys. Res. Lett*., **40**(9), 1669-1674.
386 http://doi.org/10.1002/grl.50272
387 Stocker, A. J., Honary, F., Robinson, T. R., Jones, T. B., Stubbe, P. & Kopka, H.
388 (1992). EISCAT observations of large scale electron temperature and electron
389 density perturbations caused by high power HF radio waves. *J. Atmos. Terr. Phys.*,
390 **54**(11/12), 1555-1572. http://doi.org/10.1016/0021-9169(92)90163-F
391 Utlaut, W. F. & Violette, E. J. (1972). Further observations of ionospheric
392 modification by a high-powered HF transmitter. *J. Geophys. Res.*, **77**(34),
393 6804-6818. http://doi.org/10.1029/JA077i034p06804
394 Wu, Jun, Wu, J. & Xu, Z. (2016). Results of Ionospheric Heating Experiments
395 Involving an Enhancement in Electron Density in the High Latitude Ionosphere.
396 *Plasma Sci. Technol.,* **18**(9), 890. https://doi.org/10.1088/1009-0630/18/9/03
397 Wu, Jun, Wu, J., Rietveld, M. T., Haggstrom, I., Zhao, H. & Xu, Z. (2017). The
398 behavior of electron density and temperature during ionospheric heating near the
399 fifth electron gyrofrequency. *J. Geophys. Res*. Space Physics, **122**(1), 1277-1295.
400 http://doi.org/10.1002/2016JA023121

Figure 1.

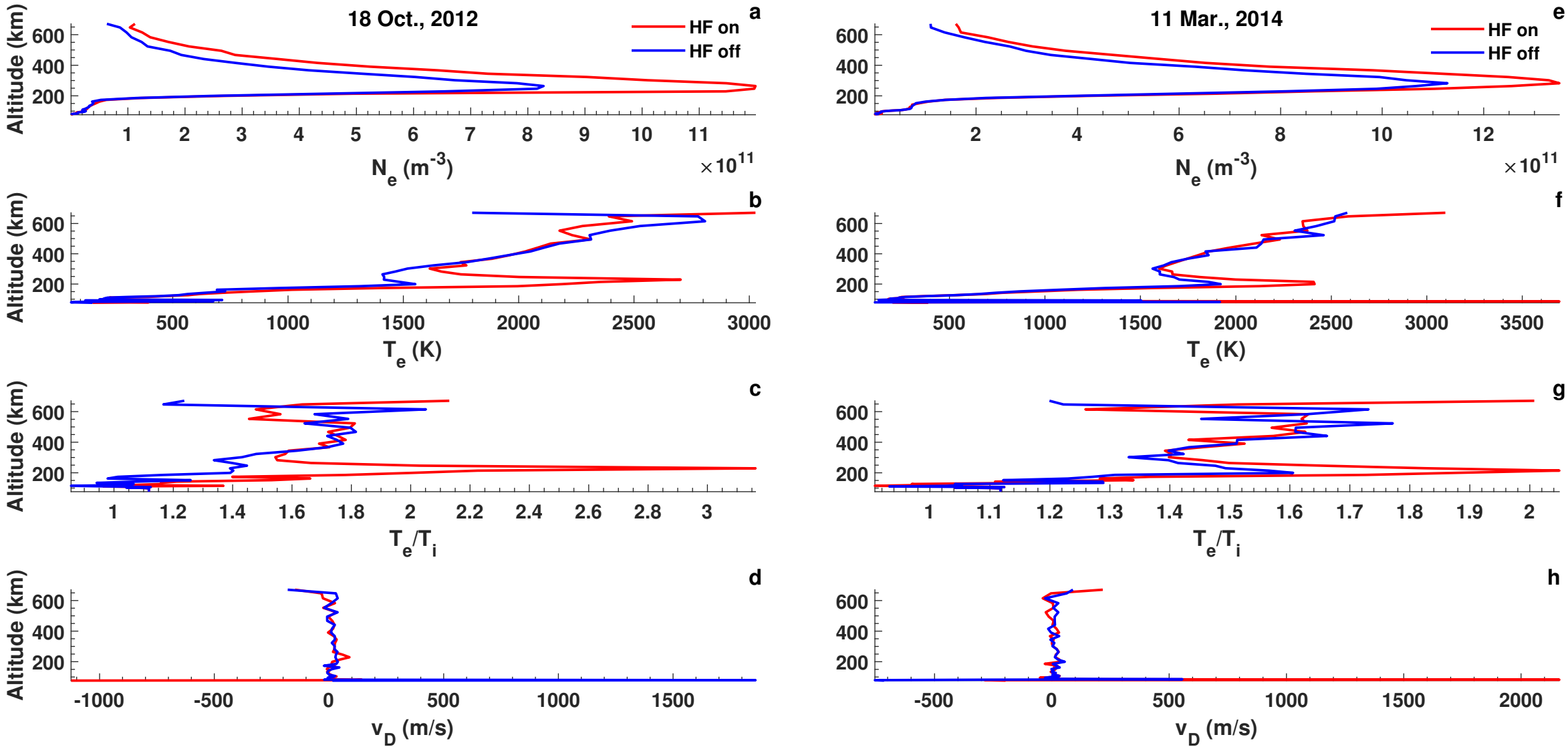
18 Oct., 2012
11 Mar., 2014
HF on
HF off
a
b
c
d
e
f
g
h
Altitude (km)
N_e (m^{-3})
$\times 10^{11}$
T_e (K)
T_e/T_i
v_D (m/s)

Figure 2.

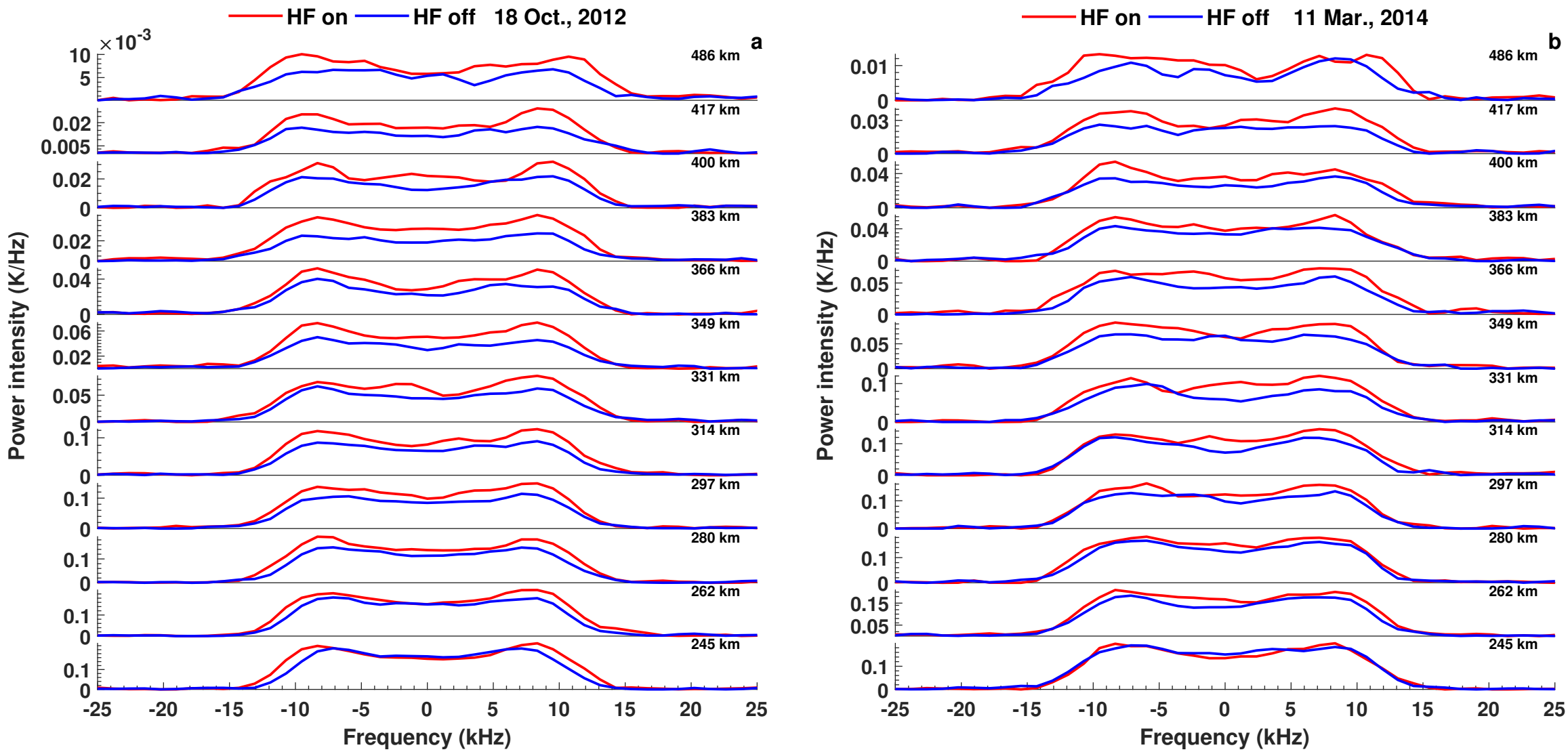
HF on
HF off
18 Oct., 2012
a
$\times 10^{-3}$
486 km
417 km
400 km
383 km
366 km
349 km
331 km
314 km
297 km
280 km
262 km
245 km
Power intensity (K/Hz)
Frequency (kHz)
HF on
HF off
11 Mar., 2014
b
Power intensity (K/Hz)
Frequency (kHz)

Figure 3.

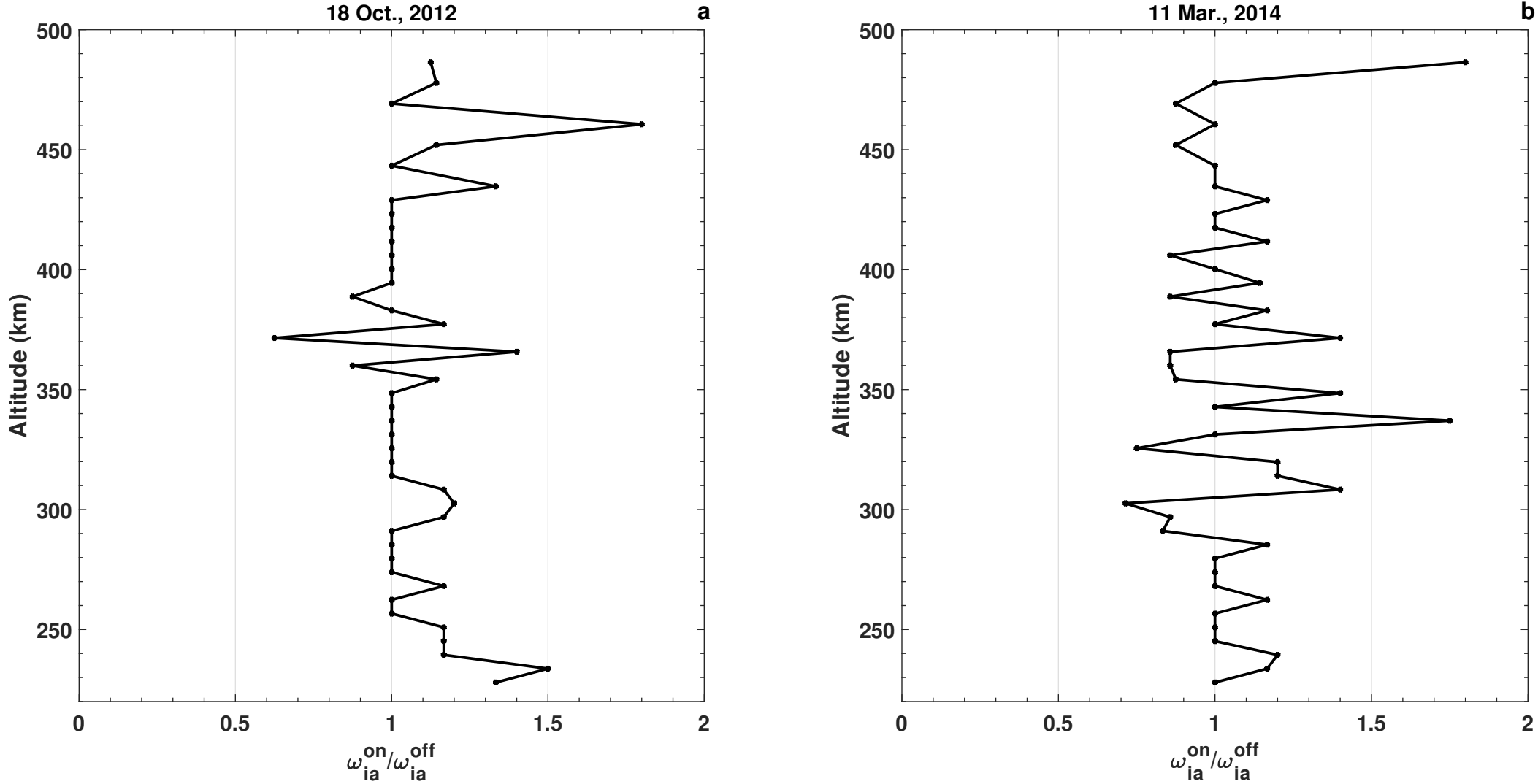
18 Oct., 2012
a
11 Mar., 2014
b
Altitude (km)
500
450
400
350
300
250
0
0.5
1
1.5
2
$\omega_{ia}^{on}/\omega_{ia}^{off}$

Figure 4.

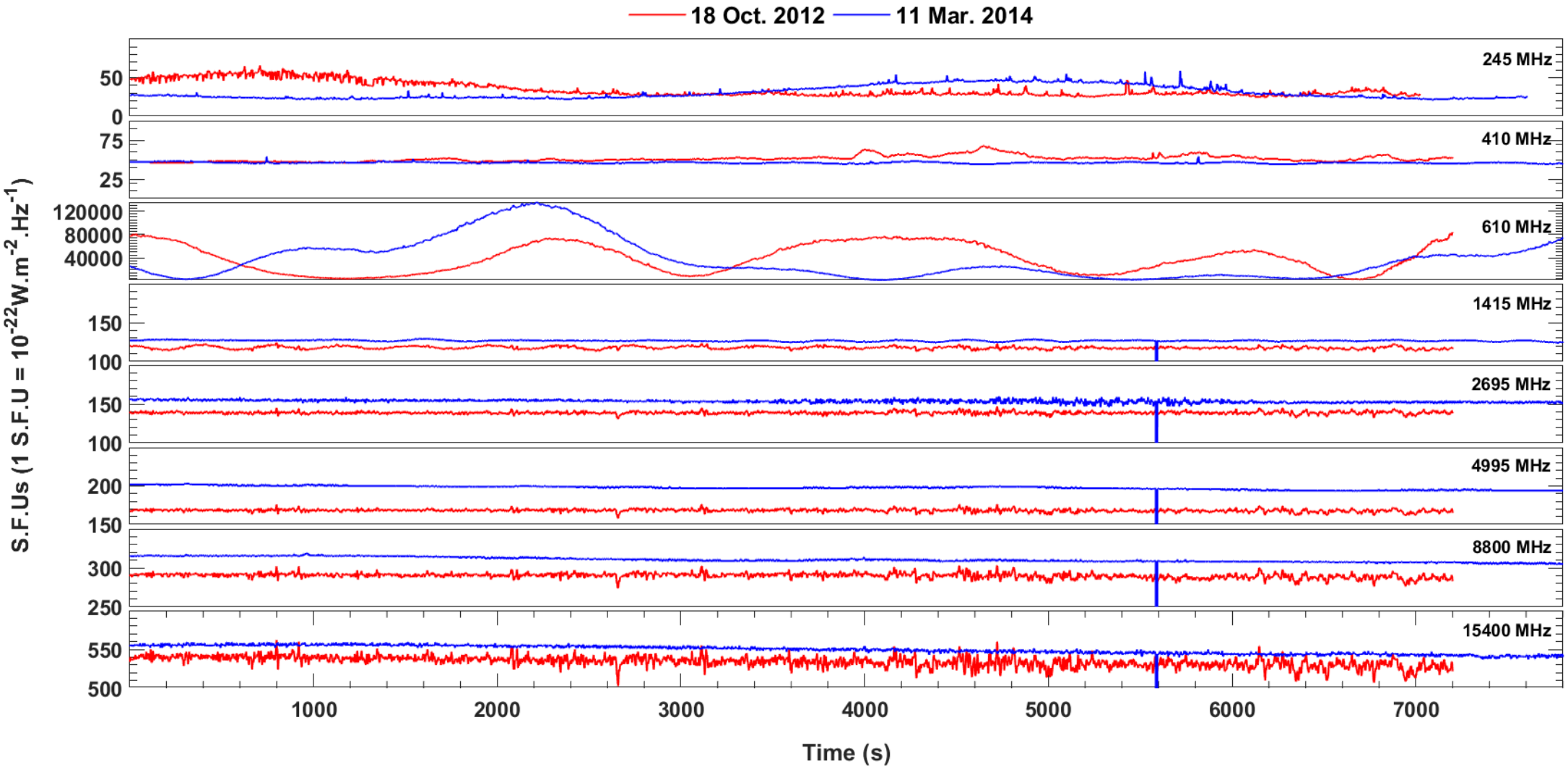
18 Oct. 2012
11 Mar. 2014
245 MHz
410 MHz
610 MHz
1415 MHz
2695 MHz
4995 MHz
8800 MHz
15400 MHz
S.F.Us (1 S.F.U = 10^-22 W.m^-2.Hz^-1)
Time (s)
1000
2000
3000
4000
5000
6000
7000